Certificate of Participation

This is to certify that:

Abdelhafid Benyounes

Participated in the "***The 2nd International Conference of Advanced Technology in Electronic and Electrical Engineering (ICATEEE2025)" held from December 10-11, 2025, at University of M'Sila, Algeria***" with a presentation entitled:

Observer-Based Sensor Fault-Tolerant Control for DC–DC Buck Converters

Co-authors: Mohammed Said Ouahabi, Said Barkat, Ismail Ghadbane, Abdelmalik Zorig.

ICATEEE 2025

December 10-11, 2025, at University of M'Sila, Algeria
https://media.univ-msila.dz/ICATEEE25/

Mohamed Boudiaf University - M'sila
The 2nd International Conference of Advanced Technology in Electronic and Electrical Engineering
ICATEEE2025
10th to 11th December 2025
M'sila
Faculty of Technology

Prof: Ismail GHADBANE

General Chair

2025 2nd International Conference of Advanced Technology in Electronic and Electrical Engineering (ICATEEE)

Observer-Based Sensor Fault-Tolerant Control for DC–DC Buck Converters

ABDELHAFID BENYOUNES
Electrical Engineering Laboratory
Faculty of Technology
University of M'sila
M'sila, Algeria
abdelhafid.benyounes@univ-msila.dz

MOHAMMED SAID OUAHABI
Electrical Engineering Laboratory
Faculty of Technology
University of M'sila
M'sila, Algeria
mohammedsaid.ouahabi@univ-msila.dz

SAID BARKAT
Electrical Engineering Laboratory
Faculty of Technology
University of M'sila
M'sila, Algeria
said.barkat@univ-msila.dz

Ismail GHADBANE
Electrical Engineering Laboratory
Faculty of Technology
University of M'sila
M'sila, Algeria
ismail.ghadbane@univ-msila.dz

Abdelmalik ZORIG
Electrical Engineering Laboratory
Faculty of Technology
University of M'sila
M'sila, Algeria
abdelmalik.zorig@univ-msila.dz

Abstract*— This paper presents an observer-based Sensor Fault-Tolerant Control scheme for a DC–DC buck converter operating under sensor faults and measurement noise. The proposed method employs a switching observer designed to estimate and compensate for sensor faults, ensuring stable converter operation even under simultaneous voltage and current sensor failures. The observer functions at the control level, serving as a protective layer that shields the double-loop control structure from faulty sensor feedback. Unlike conventional residual-based or multi-observer methods, the proposed approach utilizes a single observer that dynamically adapts to the converter's switching modes, significantly reducing computational burden while enhancing estimation accuracy. The observer design is formulated within an $\mathcal{H}_\infty$framework, and its stability conditions are derived in terms of Linear Matrix Inequalities . Simulation results conducted in MATLAB/Simulink under multiple fault cases demonstrate that the proposed FTC scheme effectively identifies and compensates sensor faults within microseconds, maintaining precise voltage regulation and current tracking under all tested conditions.

Keywords— ***DC–DC converter; sensor fault-tolerant control; switched linear system; fault estimation; LMI; power electronics***

I. INTRODUCTION

This However, DC–DC converters must satisfy application-specific performance requirements, such as fast transient response, low output voltage ripple, and robust voltage regulation under load and parameter variations [8] . Thus, a significant research efforts has gone into designing advanced control strategies to achieve optimal converter performance[9]. Traditional double-loop control structures consisting of an inner current loop and an outer voltage loop, have s been the basis for many control algorithms suggested in recent decades [10]. Both linear and nonlinear control schemes have effectively implemented to DC–DC buck converters to improve dynamic performance and steady-state accuracy [11]

However, as these converters grow more important due to their widespread adoption particularly in mission-critical systems, introduces new a challenge especially in maintaining high availability, reliability, safety, and fault diagnosis in case of failure or potential anomaly problems [12] [13]. A various fault detection and isolation schemes are designed to name a few [14], [15], [16], [17], [18]. Nevertheless, one of the most important yet often overlook issues is the possibility of unknown sensor malfunctions or failure. Sensors faults can significantly impair system performance and stability especially considering the closed loop control since the control algorithms are highly dependent on the measured values from sensors. While many studies have focused on control technique to improve the performance of the converter, most of the reported works assume non faulty sensors. Ensuring, a sensor fault tolerant control in a DC–DC converters is still a difficult , especially in the presence of strong measurement noise that can obscure fault characteristics and hinder accurate estimation[19] [20]. Consequently, developing fault tolerant strategies capable of detecting and compensating for sensor faults in real time is vital for ensuring the reliable operation of Buck converter. That can tolerate sensor fault even in the presence of noise. For instance, in [21] sensor fault detection and Fault-Tolerant Control is proposed, in which a residual based decision logic is introduced to detect the occurrence of fault however such schemes often suffer from latency due to thresholds. In [19] authors proposed residual based scheme using two crossing Extended Kalman Filters (KF) in which each observer is used to estimate a signal fault free state of the buck converter essentially using it as an analytical redundancy. however, besides the use of residual based scheme, the KF is considered one of the most computationally consuming algorithms due to the online recursive estimation. A similar scheme is proposed in using two Higher order sliding mode observer in [22], but these often suffer from chattering effects caused by measurement noise. Motivated by the aforementioned limitations, this study provides a sensor fault-tolerant control (S-FTC) technique to capable of ensuring the reliable operation of the buck converter even in the presence of severe sensor faults and abnormal measurement noise. The proposed scheme employs a single switching model-based observer designed to function at the control level to estimating the sensor faults and compensating it. Thereby the FTC scheme acts as a protective layer that keeps the control loops shielded from the adverse impacts of incorrect sensor measurement. Unlike residual-based fault identification methods that use threshold logic or multiple estimators. With the proposed

979-8-3315-6334-9/25/$31.00 ©2025 IEEE

scheme uses a single observer to simultaneously isolate and mitigate for both voltage and current sensor faults, consequently maintaining system stability and performance under faulty conditions without the need for complex fault decision mechanisms. Furthermore, the observer design ensures robustness against sensor fault by leveraging an $\mathcal{H}_\infty$ based framework, with stability guaranteed through Linear Matrix Inequalities (LMIs).

The remaining part of the present paper is organized as follows; Section II presents the modeling of the DC–DC buck converter. Section III introduces the proposed Sensor Fault-Tolerant Control scheme, including the design of the observer, the design procedure, and the control reconfiguration strategy. Section IV provides detailed simulation results that validate the effectiveness and robustness of the proposed approach under various fault scenarios. Finally, Section V concludes the paper and outlines possible directions for future work.

II. MODELING OF DC-DC BUCK CONVERTERS

The DC-DC buck converter present a significant challenge due to its inherent nonlinear and time-varying nature due to the periodic switching of semiconductor devices. A widely used method To accurately capture it dynamics is switching linear system representation in which the converter is treated as a linear time-invariant system within each switching mode, by applying Kirchhoff's circuit laws to each configuration, to each configuration, a collection of linear state-space models governed by a continuous time switching signal $\varphi(t)$ and modeled as a switched linear system of the form [15] [23]:

$$\dot{x}(t) = A_{\varphi(t)}x(t) + B_{\varphi(t)}u(t) \quad (1)$$
$$y(t) = Cx(t) \quad (2)$$

In these state space representation, $x(t)$ represents the state vector typically containing the inductor current and the capacitor voltage, $u(t)$ is the input vector. The matrices $\{A_{\varphi(t)}, B_{\varphi(t)}$ and $C\}$ are the collection of linear state space models, and $\varphi(t)$is the switching signal indicating the active mode.

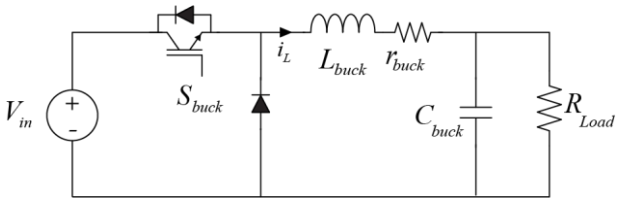

Fig. 1. Topology of a Buck DC–DC converter.

As shown in Fig. 1, the buck converter operates in Continuous Conduction Mode (CCM), where the dynamic behavior of the power stage is governed by the state of the switch S_{buck}, , controlled by a PWM signal. Accordingly, the converter dynamics can be expressed as a switched linear system of the form:

$$x(t) = \begin{bmatrix} V_{out}(t) \\ i_L(t) \end{bmatrix}, u(t) = V_{in}$$
$$\overline{A}_{\sigma(t)} = \begin{bmatrix} -\frac{1}{R_{load}C_{out}} & \frac{1}{C_{out}} \\ -\frac{1}{L} & -\frac{r_{buck}}{L} \end{bmatrix}, \overline{B}_{\sigma(t)} \begin{bmatrix} 0 \\ \frac{S_{buck}}{L} \end{bmatrix},$$
$$\overline{C} = \begin{bmatrix} 1 & 0 \\ 0 & 1 \end{bmatrix} \quad (3)$$

The possible values for switching signal $\varphi(t)$are given in Table I,

TABLE I Possible switching signal values.

$\varphi(t)$	1	2
S_{buck}	1	0

The switched state-space representation provides the foundation for developing an observer-based sensor fault control strategy, which enables fault isolation and compensation while ensuring system stability and performance.

III. SENSOR FAULT TOLERANT CONTROL SCHEME

A. Design of Observer

In DC-DC converters, sensors are employed to feedback the required information of output voltage and inductor current for the control system. However, in practice, sensor faults/failures are disposed to occur, either due to single event or accumulated degradation over time. These faults are classified as catastrophic or wear-out failures and exhibit the following fault modes [24] [25]:

Generally, these faults/failures can be mathematically modelled as affine deviations in the output, as demonstrated in [26] [27]:

$$y^f(t) = \overline{C}x(t) + \overline{Q}f^s(t) \quad (3)$$

Where $y^f(t)$ is the faulty measurements, $f^s(t) = [f_s^i \quad f_s^v]$ represents the unknown fault in the matrix. In some recent research works [28] [24] [29], it is reported that the complete sensor outage is one of the most severe faults that may lead to instability. Therefore, this paper considers all sensor faults, including complete sensor outages and noisy sensors. The observer design for the buck converter begins with formulating an augmented state-space model that incorporates the sensor fault as part of the system dynamics. the augmentation process follows the same general principle. The resulting system model, which includes the fault term (3), is expressed as follows:

$$E\dot{x}^a(t) = Ax^a(t) + B_{\varphi(t)}u(t) + Q_f f_s$$
$$y^f(t) = Cx^a(t) \quad (4)$$

Where:

$$x^a(t) = [x(t) \quad f^s(t)]^T, A = \begin{bmatrix} \overline{A} & 0 \\ 0 & I \end{bmatrix},$$
$$B_{\varphi(t)} = \begin{bmatrix} \overline{B}_{\sigma(t)} \\ 0 \end{bmatrix}, Q_f = \begin{bmatrix} 0 \\ \overline{Q}_f \end{bmatrix}, E = \begin{bmatrix} I & 0 \\ 0 & 0 \end{bmatrix}, C = [\overline{C} \quad I]$$

the following observer is constructed for the augmented system *(3)* as described by:

$$\dot{z}(t) = \mathcal{N}z(t) + \mathcal{G}_{\varphi(t)}u(t) + \mathcal{J}y^f(t)$$
$$\hat{x}^a(t) = z(t) + \mathcal{T}_2 y^f(t) \quad (5)$$

Where $\dot{z}(t)$ is the augmented state observer, $\hat{x}^a(t)$ is the estimated state vector, and $\mathcal{N}, \mathcal{J}, \mathcal{T}_2$ are constant observer gains to be determined. The proposed observer is based on unknown input observer [30]and formulated as a switching observer, tailored to account for the inherent switching dynamics of the DC-DC buck converter. Which embeds the switching behavior directly within the term $\mathcal{G}_{\varphi(t)}$ through its dependence on the input matrix $B_{\varphi(t)}$, whose structure will be determined later. This formulation ensures that the observer's internal dynamics remain consistent with the converter's active switching state, enabling dynamic adaptation to the operating mode. Consequently, the proposed switching

observer in (5) achieves accurate estimation, overcoming the limitations of classical approaches and aligning closely with the converter's real-time behavior. Denoting the estimation error as $e(t) = x^a(t) - \hat{x}^a(t)$, which can be further expanded as:

$$e(t) = x^a(t) - \hat{x}^a(t) = x^a(t) - z(t) - \mathcal{T}_2 y^f(t)$$
$$= x^a(t) - z(t) - \mathcal{T}_2 C x^a(t)$$
$$e(t) = (I - \mathcal{T}_2 C)x^a(t) - z(t) \quad (6)$$

The error *(6)* can further be expressed as:

$$e(t) = \mathcal{T}_1 E x^a(t) - z(t) \quad (7)$$

Where

$$\mathcal{T}_1 E = (I - \mathcal{T}_2 C) \quad (8)$$

The time derivative of the error *(7)* along the system-augmented dynamics *(4)* is:

$$\dot{e}(t) = \mathcal{T}_1 E \dot{x}^a(t) - \dot{z}(t) = \mathcal{T}_1 \big(A x^a(t) + B_{\varphi(t)} u(t) + Q_f f_s\big) - \mathcal{N} z(t) - \mathcal{G}_{\varphi(t)} u(t) - \mathcal{J} y^f(t) \quad (9)$$

$$\dot{e}(t) = \mathcal{T}_1 A x^a(t) + \mathcal{T}_1 B_{\varphi(t)} u(t) + \mathcal{T}_1 Q_f f_s - \mathcal{N} z(t) - \mathcal{G}_{\varphi(t)} u(t) - \mathcal{J} C x^a(t) \quad (10)$$

From (5) we have $z(t) = \hat{x}^a(t) - \mathcal{T}_2 y^f(t)$

$$\dot{e}(t) = (\mathcal{T}_1 A - \mathcal{J} C) x^a(t) + \big(\mathcal{T}_1 B_{\varphi(t)} - \mathcal{G}_{\varphi(t)}\big) u(t) + \mathcal{T}_1 Q_f f_s - \mathcal{N} \hat{x}^a(t) + \mathcal{N} \mathcal{T}_2 C x^a(t) \quad (11)$$

Since $e(t) = x^a(t) - \hat{x}^a(t), then$:

$$\dot{e}(t) = (\mathcal{T}_1 A - \mathcal{J} C + \mathcal{N} \mathcal{T}_2 C) x^a(t) + \big(\mathcal{T}_1 B_{\varphi(t)} - \mathcal{G}_{\varphi(t)}\big) u(t) + \mathcal{T}_1 Q_f f_s - \mathcal{N}(x(t) - e(t)) \quad (12)$$

Setting K=$\mathcal{J} - \mathcal{N} \mathcal{T}_2$

$$\dot{e}(t) = (\mathcal{T}_1 A - KC - \mathcal{N}) x^a(t) + \big(\mathcal{T}_1 B_{\varphi(t)} - \mathcal{G}_{\varphi(t)}\big) u(t) + \mathcal{T}_1 Q_f f_s + \mathcal{N} e(t) \quad (13)$$

If the following conditions hold:

$$\begin{cases} \mathcal{N} = \mathcal{T}_1 A - KC \\ \mathcal{G}_{\varphi(t)} = \mathcal{T}_1 B_{\varphi(t)} \\ K = \mathcal{J} - \mathcal{N} \mathcal{T}_2 \end{cases} \quad (14)$$

The state estimation error dynamics *(13)* can be reduced to:

$$\dot{e}(t) = \mathcal{N} e(t) + \mathcal{T}_1 Q_f f_s(t) \quad (15)$$

Equation *(15)* indicates that the observer defined in *(5)* design essentially involves solving *(14)*and determining a suitable gain matrix $\mathcal{N}$such that the resulting error dynamics *(15)* are stable. The design objective is to ensure the stability of the observer system matrix $\mathcal{N}$ while minimizing the influence of the unknown sensor fault $f_s(t)$on the estimation performance.

Let $V(t) = e^T \mathcal{P} e$ be a Lyapunov function candidate for the error dynamics in *(15)* where $\mathcal{P} = \mathcal{P}^T$ is a positive definite matrix with appropriate dimension, Then the time derivative of $V(t)$ is:

$$\dot{V}(t) = e^T(t) \mathcal{P} \dot{e}(t) + \dot{e}^T(t) \mathcal{P} e(t) \quad (16)$$

$$\dot{V}(t) = \Big(\mathcal{N} e(t) + \mathcal{T}_1 Q_f f_s(t)\Big)^T \mathcal{P} e(t) + e^T(t) \mathcal{P} \big(\mathcal{N} e(t) + \mathcal{T}_1 Q_f f_s\big) \quad (17)$$

$$\dot{V}(t) = e^T(t)(\mathcal{P}\mathcal{N} + \mathcal{N}^T \mathcal{P}) e(t) + 2 e(t) \mathcal{P} \mathcal{T}_1 Q_f f_s(t) \quad (18)$$

From *(18)*, it can be observed that the sensor fault $f_s(t)$ still affects the error dynamics. To achieve the asymptotic convergence of the estimation error in *(15)* while ensuring robustness against the influence of $f_s(t)$ the observer is designed to satisfy the following $\mathcal{H}_\infty$ performance index is considered, as proposed in[31]:

$$\big\|\mathcal{H}_{rf}\big\|_\infty = \sup_{\|f_s(t)\|_{\mathcal{L}_2} \neq 0} \frac{\|r(t)\|_{\mathcal{L}_2}}{\|f_s(t)\|_{\mathcal{L}_2}} \leq \sqrt{\mu} \quad (19)$$

Where$r(t) = y(t) - \hat{y}(t) = C x^a(t) - C \hat{x}^a$=Ce(t) and $\sqrt{\mu}$ is a small positive constant representing the attenuation level of the standard induced $\mathcal{L}_2$gain from the sensor fault to the estimation error. i.e. This implies a quantifiable limit on how much the sensor fault can affect the estimation error in an $\mathcal{L}_2$ sense .

The following *Theorem* provides sufficient conditions for the existence of the proposed *switching observer* in the form of *(5)* with a prescribed $\mathcal{H}_\infty$ performance index for the augmented system *(4)*.

Theorem. For a given positive constant μ, the error system (15), if there exist a symmetric positive definite matrix $P = P^T > 0$ and a matrix Φ with appropriate dimensions such that the LMI (20) hold, then the error dynamics are asymptotically stable and satisfy an $\mathcal{H}_\infty$ performance attenuation level $\sqrt{\mu}$ i.e.,

$$\big\|\mathcal{H}_{rf}\big\|_\infty \leq \sqrt{\mu}.$$

Furthermore, under these conditions, the observer (5) is feasible, with the observer gain computed as $K = P^{-1}\Phi$ and the relationships given by (14).

$$\Sigma_{III.2} = \begin{bmatrix} He(\mathcal{P}\mathcal{T}_1 A - \Phi C) & \mathcal{P}\mathcal{T}_1 Q_f & C^T \\ * & -\mu^2 I & 0 \\ * & * & -I \end{bmatrix} \leq 0 \quad (20)$$

Proof: To attain robustness to the sensor fault in the $\mathcal{L}_2$ sense, we impose the following constraint on our stability criteria:

$$\Lambda_{\text{III.2}} = r^T(t) r(t) - \mu^2 f_s^T(t) f_s(t) + \dot{V}(t) \leq 0 \quad (21)$$

Integration of both sides of the above condition with respect to *t* over the time period $[0, \infty]$ gives:

$$\int_0^\infty \big(r^T(t) r(t) - \mu^2 f_s^T(t) f_s(t)\big) dt + V(\infty) - V(0) \quad (22)$$

Assuming a zero initial-condition $V(0) = 0$ and recognizing that the Lyapunov function is always non-negative $V(\infty) \geq 0$ e the previous inequality simplifies to:

$$\sqrt{\int_0^\infty r^T(t) r(t) dt} \leq \mu^2 \sqrt{\int_0^\infty f^T(t) f(t) dt} \quad \forall t > 0 \quad (23)$$

Therefore, we have

$$\frac{\sqrt{\int_0^\infty r^T(t) r(t) dt}}{\sqrt{\int_0^\infty f^T(t) f(t) dt}} \leq \mu^2 \qquad \forall t > 0 \quad (24)$$

or equivalently

$$\big\|\mathcal{H}_{rf}\big\|_\infty \leq \sqrt{\mu}. \quad (25)$$

In other words, *(21)* enforces the minimization of the worst case effect of the sensor fault on the estimation error *(15)*. Therefore, from *(21)* and by using *(18)* we obtain:

$$\Lambda_{III.2} = r^T(\tau) r(\tau) - \mu^2 f_s^T(\tau) f_s(\tau) + \dot{V}(\tau) \leq e^T(t)(\mathcal{P}\mathcal{N} + \mathcal{N}^T \mathcal{P}) e(t) + 2 e(t) \mathcal{P} \mathcal{T}_1 Q_f f_s(t) + e^T(t) C^T C e(t) - \mu^2 f_s^T(\tau) f_s(\tau) \quad (26)$$

Using $\mathcal{N} = \mathcal{T}_1 A - KC$

$$\Lambda_{III.2} \le e^T(t)\big(\mathcal{P}\mathcal{T}_1 A - \mathcal{P}KC + A^T {\mathcal{T}_1}^T \mathcal{P} - C^T K^T \mathcal{P}\big)e(t)$$
$$+2e(t)\mathcal{P}\mathcal{T}_1 Q_f f_s(t) + e^T(t)C^T Ce(t) - \mu^2 f_s^T(\tau) f_s(\tau) \quad (27)$$

Consequently, the expression is

$$\Lambda_{III.2} \le [e(t) \quad f_s(t)]^T \left(\begin{bmatrix} He(\mathcal{P}\mathcal{T}_1 A - \mathcal{P}KC) & \mathcal{P}\mathcal{T}_1 Q_f \\ * & 0 \end{bmatrix} + \begin{bmatrix} C^T C & 0 \\ * & -\mu^2 I \end{bmatrix} \right) \begin{bmatrix} e(t) \\ f_s(t) \end{bmatrix} \quad (28)$$

It follows that

$$\Lambda_{III.2} \le [e(t) \quad f_s(t)]^T \left(\begin{bmatrix} He(\mathcal{P}\mathcal{T}_1 A - \mathcal{P}KC) & \mathcal{P}\mathcal{T}_1 Q_f \\ * & -\mu^2 I \end{bmatrix} + [C^T \quad 0] I \begin{bmatrix} C \\ 0 \end{bmatrix} \right) \begin{bmatrix} e(t) \\ f_s(t) \end{bmatrix} \quad (29)$$

By applying Schur-complement,

$$\Lambda_{III.2} \le$$

$$[e(t) \quad f_s(t)]^T \left(\overbrace{\begin{bmatrix} He(\mathcal{P}\mathcal{T}_1 A - \mathcal{P}KC) & \mathcal{P}\mathcal{T}_1 Q_f & C^T \\ * & -\mu^2 I & 0 \\ * & * & -I \end{bmatrix}}^{\Sigma_{III.2}} \right) \begin{bmatrix} e(t) \\ f_s(t) \end{bmatrix}$$

(30)

Notice that the above matrix inequality is nonlinear by setting $\phi = \mathcal{P}K$ consequently we find the LMI in *(20)*. therefore If the condition *(20)* is feasible, Then $r^T(t)r(t) - \mu^2 f_s^T(t) f_s(t) + \dot{V}(t) \le 0$ Thus, the observer error dynamics is asymptotically stable with the prescribed attenuation level defined in *(19)* enforces the minimization of the worst case effect of the sensor fault on the estimation error if *(15)* is satisfied. Thus, the observer error dynamics is asymptotically stable with the prescribed $\mathcal{H}_\infty$ performance attenuation level $\sqrt{\mu}$ subject to $\|r(t)\|_{\mathcal{L}_2} \le \sqrt{\mu}\|f_s(t)\|_{\mathcal{L}_2}$.

This completes the proof of Theorem 1.■

B. Design procedure

Based on the previous subsection, the design procedure of the switched observer in *(5)* for fault estimation can be summarized as follows: for the buck type converter

1. Construct the augmented system in the form of *(4)*.
2. Select the matrices $\mathcal{T}_1$ and $\mathcal{T}_2$ in the form of *(14)*.

these matrices are computed to satisfy the following decoupling condition:

$$\mathcal{T}_1 E + \mathcal{T}_2 C = I \quad (31)$$

Which is equivalent to

$$[\mathcal{T}_1 \quad \mathcal{T}_2] \begin{bmatrix} E \\ C \end{bmatrix} = I \quad (32)$$

Since the block matrix $\begin{bmatrix} E \\ C \end{bmatrix}$ is non-square, the solution is obtained using the Moore–Penrose pseudoinverse. Consequently, the transformation matrices are computed as:

$$[\mathcal{T}_1 \quad \mathcal{T}_2] = \begin{bmatrix} E \\ C \end{bmatrix}^\dagger = \left(\begin{bmatrix} E \\ C \end{bmatrix}^T \begin{bmatrix} E \\ C \end{bmatrix} \right)^{-1} \begin{bmatrix} E \\ C \end{bmatrix}^T \quad (33)$$

Where $\begin{bmatrix} E \\ C \end{bmatrix}^\dagger$ denotes the pseudoinverse of the stacked matrix.

3. Solve the LMI condition in *(20)* to obtain matrices Φ, and P, ensuring the observer satisfies the stability and$\mathcal{H}_\infty$ performance constraints. then calculate the gain $K = \mathcal{P}^{-1}\phi$.
4. Calculation $\mathcal{N}$ of $\mathcal{J}$ and using *(14)*.
5. Implement the switched observer and obtain the fault estimation.

the implementation of the proposed observer requires dynamic adaptation of the gain matrix $\mathcal{G}_{\varphi(t)}$, computed as:

$$\mathcal{G}_{\varphi(t)} = \mathcal{T}_1 B_{\varphi(t)} \quad (34)$$

where $\mathcal{T}_1$ is the design matrix obtained in Step 2, and $B_{\varphi(t)}$ denotes the system input matrix. the DC-DC buck converter under consideration exhibits switching dynamics, making $B_{\varphi(t)}$ a function of the switching signal S_{buck}. Consequently, in the actual implementation, $\mathcal{G}_{\varphi(t)}$ must also dynamically adapt to the switching signal, ensuring consistency between the observer structure and the converter's operating mode.

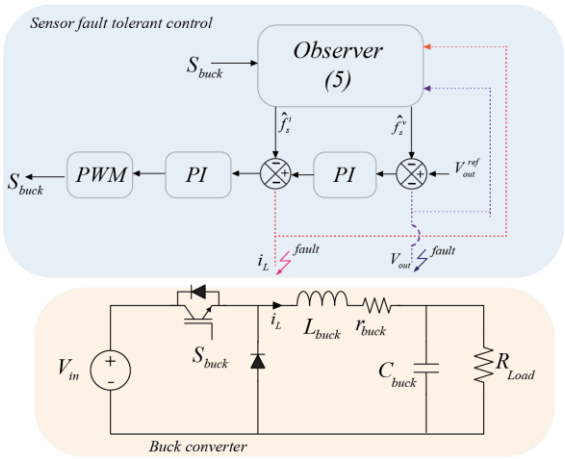

Fig. 2. FTC scheme for the buck converter.

C. Control reconfiguration

The block diagram the overall FTC scheme for the buck converter is depicted in Fig. 2. based on the proposed Switching Observer. The adopted control is cascaded PI control architecture, where the inner current loop is designed to operate with a bandwidth approximately eight times higher than that of the outer voltage loop. To ensure fast current dynamics while maintaining overall closed-loop stability, the bandwidth of the inner loop is further constrained to be one-tenth of the converter's switching frequency[32]. The fault compensation is achieved at the controller level by continuously compensating the faulty sensor measurements using fault estimates provided by the Switching Observer. Unlike conventional residual-based FTC approaches, which rely on explicit fault detection, isolation, and subsequent switching logic, often leading to delays and potential false alarms, as shown in Fig. 2. Consequently, when a fault occurs, the FTC promptly compensates for its effect, while in the absence of faults, the estimation remains near zero, thereby enabling seamless operation without introducing control discontinuities.

IV. SIMULATION RESULTS

To evaluate the performance and effectiveness of the proposed observer-based sensor fault-tolerant control (S-FTC) scheme, a buck converter was modeled and simulated in MATLAB/Simulink operating in CCM. with a step change in load is introduced to assess the FTC response under varying operating conditions. The controller parameters of DC-DC converters are selected based on conventional bandwidth separation, ensuring that the inner current loop bandwidth is significantly faster than the outer voltage loop, as detailed in

section II. The observer parameters were obtained by solving the LMI (20) with an attenuation levels set to $\sqrt{\mu} = 0.001$. To comprehensively evaluate the fault-tolerant performance, 3 test cases were formulated. Each case introduces different types of sensor faults with distinct activation intervals to emulate realistic and challenging operating conditions, including both simultaneous and sequential faults.

Test Case 1: Bias Faults

Positive and negative bias faults were introduced in both the voltage and current sensors. The voltage sensor experienced a sensor fault $f_s^v(t) = -10 + 8sin(6\pi t)$, and the current sensors during t={0.2,0.6}s and t={0.7,1.1}s , subsequently, both sensors experienced simultaneous sensors during t= {1.2, 1.7} s mathematically express as $f_s^v(t) = 10 + 8sin(6\pi t)$, and $f_s^i(t) = -1 + sin(8\pi t)$

Test Case 2 : Time-Varying and Random Noise Faults

To evaluate robustness under dynamic disturbances, time-varying faults and random noise faults were introduced. The voltage sensor was affected by a slowly varying sinusoidal fault $f_s^v(t) = 20\,sin(12\pi t)$,while the current sensor experienced similar time varing fault of theform $f_s^i = 1.4\,sin(14\pi t)$ both during t= {0.2, 0.6} s. *In addition, a random noise fault* $f_s^v = v_k\sqrt{0.0001}, with v_k \sim \mathcal{N}(0,1)$ *and* $f_s^i = w_k\sqrt{0.00001}$ *with* $w_k \sim \mathcal{N}(0,1)$ *is applied to the voltage and current sensors during t={1.2, 1.7} s and t={0.7, 1.1} s, respectively.*

Test Case 3 open-Circuit Fault and Sudden Sensor Fault

In the final test, the current sensor was subject to complete sensor failure with the measured current is zero, and sudden complete sensor failure is set to occur at the same instant as the load variation, exacerbating the situation at t=0.9s in the voltage sensor.

The results for these scenarios are illustrated in Fig. 3 to 5. Each figure contains the measured inductor current $i_L^{measured}(t)$, and the output voltage $V_o^{measured}(t)$ along with their corresponding sensor fault $f_s^i(t), f_s^v(t)$ and sensor fault estimation $\hat{f}_s^i(t), \hat{f}_s^v(t)$ as well as the reconfigured inductor current denoted $i_L^{compensated}(t)$ and output voltage denoted $V_o^{compensated}(t)$,

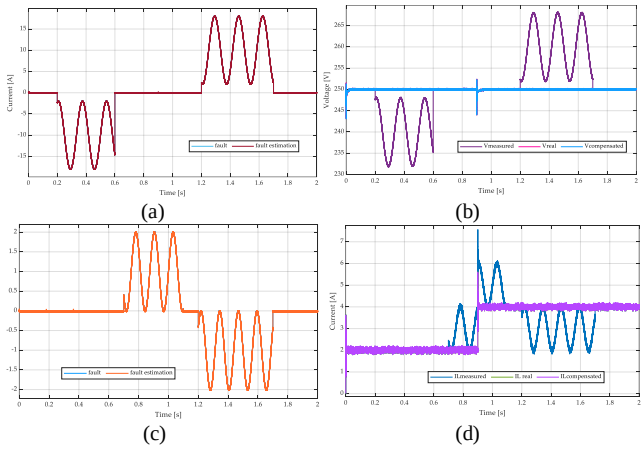

(a) (b) (c) (d)

FIG.3 results of case 1: (a) voltage sensor fault and its estimation, (b) faulty, actual, and the reconfigured value of the output voltage, (c) inductor sensor fault and its estimation, (d) faulty, actual and reconfigured value of the inductor current.

As demonstrated in (a) and(c) of Fig.3 to 5 the switching observer provides a highly accurate estimation of the sensor faults $\hat{f}_s^i(t), \hat{f}_s^v(t)$ which closely track their actual injected values $f_s^i(t), f_s^v(t)$ across all fault types. This precision is maintained during start-up and load changes, as well as during abrupt fault occurrences.

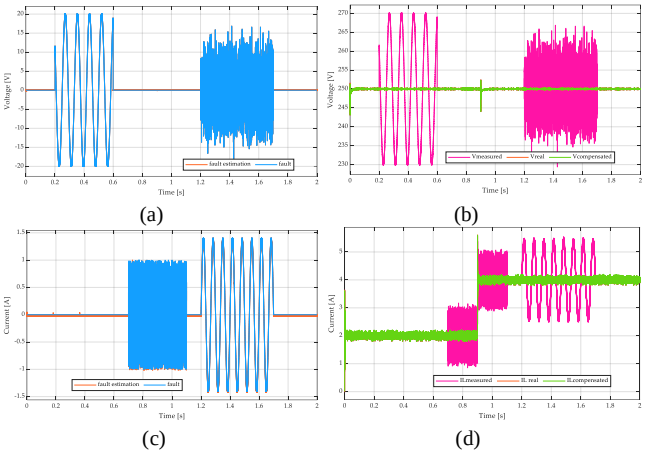

(a) (b) (c) (d)

FIGURE 4 results of case 2: (a) voltage sensor fault and its estimation, (b) faulty, actual, and the reconfigured value of the output voltage, (c) inductor sensor fault and its estimation, (d) faulty, actual and reconfigured value of the inductor current.

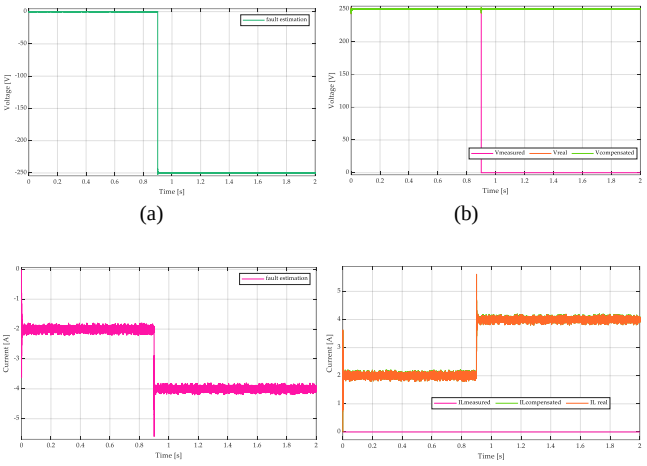

(a) (b) (c) (d)

FIGURE 5 results of case: 3 (a) voltage sensor fault estimation, (b) faulty, actual, and the reconfigured value of the output voltage, (c) inductor sensor fault estimation, (d) faulty, actual and reconfigured value of the inductor current.

The estimation errors consistently maintain low, with maximum values of approximately 0.02 A for the current and 0.05 V for the voltage, ensuring a robust basis for compensation. The effectiveness of the proposed observer based sensor FTC effectively mitigate sensor faults within *1 μs* in the buck converter even if the sensor faults occurred concurrently, as presented in (b) and (d) of Fig.3 through 5 across all faults as the buck converter continues to function normally without performance degradation.as can be seen in the compensated output voltage $V_o^{compensated}(t)$ and inductor current $i_L^{compensated}(t)$ waveforms consistently overlap their true values throughout all four scenarios.

In conclusion, the results presented in Fig.3 to 5 unequivocally demonstrate that the proposed observer provides a highly effective sensor FTC solution for the buck converter. The scheme's ability to provide rapid, accurate, and seamless fault mitigation across various fault types and operational conditions confirms its effectiveness in ensuring the stable and reliable operation of the converter.

V. CONCLUSION

This paper has proposed an observer-based sensor fault-tolerant control scheme for DC–DC buck converters. the proposed method estimates and compensate sensor faults, including bias, noise, sudden sensor fault and complete sensor failure. the observer design, established within an $\mathcal{H}_\infty$based LMI framework, guarantees stability and robustness against sensor disturbances. Simulation results have validated that the proposed FTC approach can effectively mitigate multiple simultaneous sensor faults with minimal delay and without degrading converter performance. this method offers faster response, lower computational complexity, and seamless control reconfiguration. Future work will focus on experimental validation on hardware.

REFERENCES

[1]D. Shahzad, S. Pervaiz, N. A. Zaffar, and K. K. Afridi, "GaN-based high-power-density AC–DC–AC converter for single-phase transformerless online uninterruptible power supply," *IEEE Transactions on Power Electronics*, vol. 36, no. 12, pp. 13968-13984, 2021.

[2]H. Zhao, Y. Shen, W. Ying, S. S. Ghosh, M. R. Ahmed, and T. Long, "A single-and three-phase grid compatible converter for electric vehicle on-board chargers," *IEEE Transactions on Power Electronics*, vol. 35, no. 7, pp. 7545-7562, 2019.

[3]S. P. Barave and B. H. Chowdhury, "Hybrid AC/DC power distribution solution for future space applications," in *2007 IEEE Power Engineering Society General Meeting*, 2007: IEEE, pp. 1-7.

[4]A. Emadi, S. S. Williamson, and A. Khaligh, "Power electronics intensive solutions for advanced electric, hybrid electric, and fuel cell vehicular power systems," *IEEE Transactions on power electronics*, vol. 21, no. 3, pp. 567-577, 2006.

[5]H. Zhang, F. Mollet, C. Saudemont, and B. Robyns, "Experimental validation of energy storage system management strategies for a local dc distribution system of more electric aircraft," *IEEE Transactions on Industrial Electronics*, vol. 57, no. 12, pp. 3905-3916, 2010.

[6]J. G. Ciezki and R. W. Ashton, "Selection and stability issues associated with a navy shipboard DC zonal electric distribution system," *IEEE Transactions on power delivery*, vol. 15, no. 2, pp. 665-669, 2002.

[7]S. Augustine, S. Brahma, J. E. Quiroz, and M. J. Reno, "DC microgrid protection: Review and challenges," 2018.

[8]E. Hernández-Márquez, R. Silva-Ortigoza, J. R. García-Sánchez, M. Marcelino-Aranda, and G. Saldaña-González, "A DC/DC Buck-Boost converter–inverter–DC motor system: Sensorless passivity-based control," *IEEE Access*, vol. 6, pp. 31486-31492, 2018.

[9]H.-H. Park and G.-H. Cho, "A DC–DC converter for a fully integrated PID compensator with a single capacitor," *IEEE Transactions on Circuits and Systems II: Express Briefs*, vol. 61, no. 8, pp. 629-633, 2014.

[10]S. Bacha, I. Munteanu, and A. I. Bratcu, *Power electronic converters: modeling and control*. Springer, 2014.

[11]Y. Yin *et al.*, "Advanced control strategies for DC–DC buck converters with parametric uncertainties via experimental evaluation," *IEEE Transactions on Circuits and Systems I: Regular Papers*, vol. 67, no. 12, pp. 5257-5267, 2020.

[12]S. S. Khan and H. Wen, "A comprehensive review of fault diagnosis and tolerant control in DC-DC converters for DC microgrids," *IEEE Access*, vol. 9, pp. 80100-80127, 2021.

[13]G. K. Kumar and D. Elangovan, "Review on fault-diagnosis and fault-tolerance for DC–DC converters," *IET Power Electronics*, vol. 13, no. 1, pp. 1-13, 2020.

[14]E. Ribeiro, A. J. M. Cardoso, and C. Boccaletti, "Open-circuit fault diagnosis in interleaved DC–DC converters," *IEEE transactions on power electronics*, vol. 29, no. 6, pp. 3091-3102, 2013.

[15]J. Poon, P. Jain, I. C. Konstantakopoulos, C. Spanos, S. K. Panda, and S. R. Sanders, "Model-based fault detection and identification for switching power converters," *IEEE Transactions on Power Electronics*, vol. 32, no. 2, pp. 1419-1430, 2016.

[16]M. Li, D. Yu, S. S. Yu, X. Li, and H. Geng, "Enhanced Fault Detection, Localization, and Tolerance Strategy for Dual Active Bridge DC–DC Converters Through Frequency-Domain Analysis of Remote Voltage," *IEEE Transactions on Industrial Electronics*, 2025.

[17]B. Kim, M. Kim, W. Kim, and H.-P. Park, "DC Series Arc Fault Detection Capability With Frequency Spectrum Analysis Using LCL-Type Boost Converter for PV Applications," *IEEE Transactions on Energy Conversion*, 2025.

[18]H.-P. Park, S.-J. Chang, J.-Y. Park, M. Kim, W. Kim, and S. Chae, "DC series arc fault detection method with resonant filter design for PV systems," *IEEE Transactions on Power Electronics*, vol. 39, no. 11, pp. 14240-14250, 2024.

[19]S. Schmidt, J. Oberrath, and P. Mercorelli, "A sensor fault detection scheme as a functional safety feature for dc-dc converters," *Sensors*, vol. 21, no. 19, p. 6516, 2021.

[20]M. Schimmack and P. Mercorelli, "An adaptive derivative estimator for fault-detection using a dynamic system with a suboptimal parameter," *Algorithms*, vol. 12, no. 5, p. 101, 2019.

[21]J. Li, K. Pan, Q. Su, and X.-Q. Zhao, "Sensor fault detection and fault-tolerant control for buck converter via affine switched systems," *IEEE Access*, vol. 7, pp. 47124-47134, 2019.

[22]D. Narzary and K. C. Veluvolu, "Higher order sliding mode observer-based sensor fault detection in DC microgrid's buck converter," *Energies*, vol. 14, no. 6, p. 1586, 2021.

[23]D. Belkhiat, N. Messai, and N. Manamanni, "Design of a robust fault detection based observer for linear switched systems with external disturbances," *Nonlinear Analysis: Hybrid Systems*, vol. 5, no. 2, pp. 206-219, 2011.

[24]S. K. Kommuri, M. Defoort, H. R. Karimi, and K. C. Veluvolu, "A robust observer-based sensor fault-tolerant control for PMSM in electric vehicles," *IEEE Transactions on Industrial Electronics*, vol. 63, no. 12, pp. 7671-7681, 2016.

[25]S. Xu, Z. Zheng, W. Huang, Y. Liu, and H. Chen, "Current Sensor Fault Estimation and Fault Tolerance of Grid-Connected Three-Level NPC Inverter Based on Reduced-Order Observer," in *2023 6th International Conference on Robotics, Control and Automation Engineering (RCAE)*, 2023: IEEE, pp. 234-238.

[26]M. Huang, L. Ding, W. Li, C.-Y. Chen, and Z. Liu, "Distributed observer-based H∞ fault-tolerant control for DC microgrids with sensor fault," *IEEE Transactions on Circuits and Systems I: Regular Papers*, vol. 68, no. 4, pp. 1659-1670, 2021.

[27]N. Vafamand, M. M. Arefi, M. H. Asemani, M. S. Javadi, F. Wang, and J. P. Catalão, "Dual-EKF-based fault-tolerant predictive control of nonlinear DC microgrids with actuator and sensor faults," *IEEE Transactions on Industry Applications*, vol. 58, no. 4, pp. 5438-5446, 2022.

[28]A. Afshari, M. Karrari, H. R. Baghaee, and G. B. Gharehpetian, "Distributed fault-tolerant voltage/frequency synchronization in autonomous AC microgrids," *IEEE Transactions on Power Systems*, vol. 35, no. 5, pp. 3774-3789, 2020.

[29]B. Tabbache, M. E. H. Benbouzid, A. Kheloui, and J.-M. Bourgeot, "Virtual-sensor-based maximum-likelihood voting approach for fault-tolerant control of electric vehicle powertrains," *IEEE transactions on vehicular technology*, vol. 62, no. 3, pp. 1075-1083, 2012.

[30]M. Darouach, "Complements to full order observer design for linear systems with unknown inputs," *Applied Mathematics Letters*, vol. 22, no. 7, pp. 1107-1111, 2009.

[31]R. Raoufi, H. Marquez, and A. Zinober, "$\mathcal{H}\infty$ sliding mode observers for uncertain nonlinear Lipschitz systems with fault estimation synthesis," *International Journal of Robust and Nonlinear Control*, vol. 20, no. 16, pp. 1785-1801, 2010.

[32]A. Sharida, S. Bayhan, and H. Abu-Rub, "Fault-tolerantself-tuning control for three-phase three-level T-type rectifier," *IEEE Transactions on Power Electronics*, vol. 38, no. 6, pp. 7049-7058, 2023.